LETTER

doi:10.1038/nature12715

Attention to eyes is present but in decline in 2–6-month-old infants later diagnosed with autism

Warren Jones[1,2,3] & Ami Klin[1,2,3]

Deficits in eye contact have been a hallmark of autism[1,2] since the condition's initial description[3]. They are cited widely as a diagnostic feature[4] and figure prominently in clinical instruments[5]; however, the early onset of these deficits has not been known. Here we show in a prospective longitudinal study that infants later diagnosed with autism spectrum disorders (ASDs) exhibit mean decline in eye fixation from 2 to 6 months of age, a pattern not observed in infants who do not develop ASD. These observations mark the earliest known indicators of social disability in infancy, but also falsify a prior hypothesis: in the first months of life, this basic mechanism of social adaptive action—eye looking—is not immediately diminished in infants later diagnosed with ASD; instead, eye looking appears to begin at normative levels prior to decline. The timing of decline highlights a narrow developmental window and reveals the early derailment of processes that would otherwise have a key role in canalizing typical social development. Finally, the observation of this decline in eye fixation—rather than outright absence—offers a promising opportunity for early intervention that could build on the apparent preservation of mechanisms subserving reflexive initial orientation towards the eyes.

Autism Spectrum Disorders (ASDs) affect approximately 1 in every 88 individuals[6]. These disorders are lifelong, believed to be congenital, and are among the most highly heritable of psychiatric conditions[7]. However, the genetic heterogeneity of ASD—with estimates suggesting as many as three- to five-hundred distinct genes impacting aetiology[8]—poses a stark challenge for understanding the biology of the condition: with so many different 'causes', a key question is how that genetic heterogeneity can be instantiated into common forms of disability.

One answer is that although the specific biological mechanisms may vary (in genes or pathways affected, in dosage or in timing), any such disruptions will contribute to an individual deviation from normative developmental processes[9,10]; the mechanisms may initially be different, but a divergence from typical development is shared. In this way, widely varying initial liabilities can be converted into similar manifestations of impairment, giving rise to the spectrum of social disability we then call 'autism'.

In typical development, the processes of normative social interaction are extremely early-emerging: from the first hours and weeks of life, preferential attention to familiar voices[11], faces[12], face-like stimuli[13] and biological motion[14] guide typical infants[15]. These processes are highly conserved phylogenetically[16] and lay the foundation for iterative specialization of mind and brain[17], entraining babies to the social signals of their caregivers[11–14,18].

In the current study, we tested the extent to which measures of these early-emerging normative processes may reveal disruptions in ASD at a point prior to the manifestation of overt symptoms. We measured preferential attention to the eyes of others, a skill present in typical infants[12] but significantly impaired in 2-year-olds with ASD[2]. We proposed that in infants later diagnosed with ASD, preferential attention to others' eyes might be diminished from birth onwards[2,3,17].

Data were collected at 10 time points: at months 2, 3, 4, 5, 6, 9, 12, 15, 18 and 24. We studied 110 infants, enrolled as risk-based cohorts: $n = 59$ at high-risk for ASD (full siblings of a child with ASD[19]) and $n = 51$ at low-risk (without first-, second- or third-degree relatives with ASD). Diagnostic status was ascertained at 36 months. For details on study design, clinical characterization of participants, and experimental procedures, see Methods and Supplementary Information.

Of the high-risk infants, 12 met criteria for ASD[20] (10 males, 2 females), indicating a conversion rate of 20.3%[19]. One child from the low-risk cohort was also diagnosed with ASD. Given the small number of girls in the ASD group, we constrained current analyses to males only, 11 ASD (10 from the high-risk cohort and 1 from the low-risk), and 25 typically developing (all from the low-risk cohort).

At each testing session, infants viewed scenes of naturalistic caregiver interaction (Fig. 1a, b) while their visual scanning was measured with eye-tracking equipment. The 36 typically developing and ASD children viewed 2,384 trials of video scenes.

Control comparisons tested for between-group differences in attention to task and completion of procedures. There were no between-group differences in duration of data collected per child (typically developing = 71.25 (27.66) min, ASD = 64.16 (30.77) min, data given as mean (standard deviation), with $t_{34} = 0.685$, $P = 0.498$; two-sample t-test with 34 degrees of freedom, equal variances); or in the distribution of ages at which successful data collection occurred ($k = 0.0759$, $P = 0.9556$; two-sample Kolmogorov–Smirnov test). Calibration accuracy was not significantly different between groups: either cross-sectionally, at any data collection session (all $P > 0.15$, $t < 1.44$; mean $P = 0.428$); or longitudinally, as either a main effect of diagnosis ($F_{1,2968.336} = 0.202$, $P = 0.65$) or as an interaction of diagnosis by time ($F_{1,130.551} = 0.027$, $P = 0.87$) (by hierarchical linear modelling; see Methods, Supplementary Information and Extended Data Fig. 8).

We then measured percentage of visual fixation time to eyes, mouth, body and object regions (Fig. 1c). For each child, during each video, these measures served as the dependent variables for longitudinal analyses. Longitudinal analyses were conducted by functional data analysis (FDA)[21] and principal analysis by conditional expectation (PACE)[22] (examples in Fig. 1d, e), and were repeated with traditional growth curve analysis using hierarchical linear modelling (HLM)[23].

Growth curves for normative social engagement show broad developmental change in typically developing infants during the first 2 years of life (Fig. 2a and Extended Data Figs 2, 4 and 7). From 2 to 6 months, typically developing infants look more at the eyes than at mouth, body, or object regions (all $F_{1,23} > 15.74$, $P < 0.001$, by functional analysis of variance (functional ANOVA)[21]) (Fig. 2a, e). Mouth fixation increases during the first year and peaks at approximately 18 months (Fig. 2a, f). Fixation on body and object regions declines sharply throughout the first year, reaching a plateau between 18 and 24 months (Fig. 2a, g, h), with greater fixation on body than on object regions at all time points ($F_{1,23} = 18.02$, $P < 0.001$).

In infants later diagnosed with ASD, growth curves of social visual engagement follow a different developmental course (Fig. 2b and

[1]Marcus Autism Center, Children's Healthcare of Atlanta, Atlanta, Georgia 30329, USA. [2]Division of Autism & Related Disabilities, Department of Pediatrics, Emory University School of Medicine, Atlanta, Georgia 30022, USA. [3]Center for Translational Social Neuroscience, Emory University, Atlanta, Georgia 30022, USA.

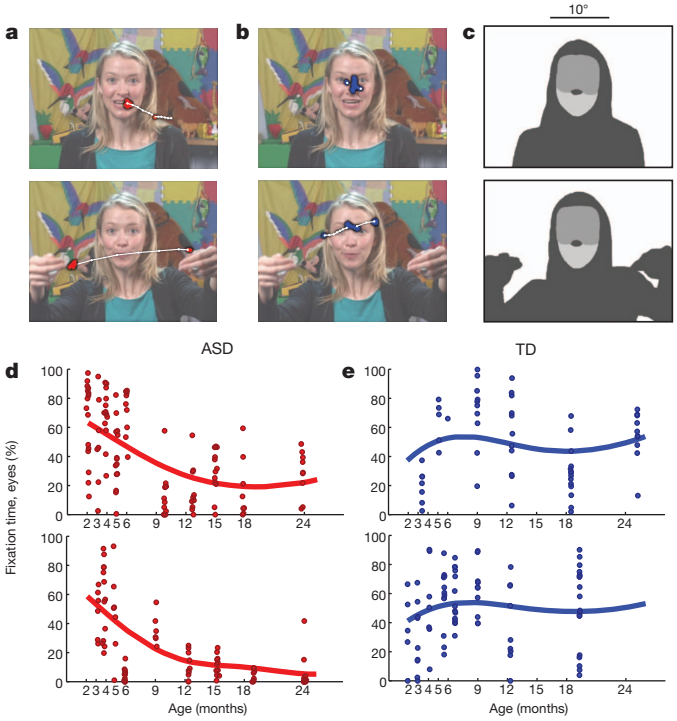

Figure 1 | Example stimuli, visual scanpaths, regions-of-interest, and longitudinal eye-tracking data from 2 until 24 months of age. **a**, Data from a 6-month-old infant later diagnosed with ASD, red. **b**, Data from a typically developing (TD) 6-month-old infant, blue. Two seconds of eye-tracking data are overlaid on each still image, onscreen at the midpoint of the data sample. Saccades are plotted as thin white lines with white dots; fixation data are plotted as larger coloured dots. **c**, Corresponding regions of interest for each image in **a** and **b**, shaded to indicate eye, mouth, body and object regions. **d**, **e**, Trial data with FDA curve fits plotting percentage of total fixation time on eyes, from 2 until 24 months of age, for two children with ASD (**d**) and two TD children (**e**).

Extended Data Figs 2, 5 and 7). From 2 until 24 months of age, eye fixation declines, arriving at a level that is approximately half that of typically developing children by 24 months (Fig. 2e). Fixation on others' mouths increases from month 2 until approximately month 18 (Fig. 2f). Fixation on others' bodies declines in children with ASD, but at less than half the rate of typically developing children, stabilizing at a level 25% greater than typical (Fig. 2g). Object fixation also declines more slowly in children with ASD, and increases during the second year (Fig. 2h), rising by 24 months to twice the level of typical controls.

Between-group comparison of entire 2- to 24-month growth curves by functional ANOVA[21] reveals significant differences in eye fixation (Fig. 2e, $F_{1,34} = 11.90$, $P = 0.002$), in body fixation (Fig. 2g, $F_{1,34} = 10.60$, $P = 0.003$), and in object fixation (Fig. 2h, $F_{1,34} = 12.08$, $P = 0.002$), but not in mouth fixation (Fig. 2f, $F_{1,34} = 0.002$, $P = 0.965$) (Bonferroni corrections for multiple comparisons, $\alpha = 0.0125$). Related analyses, including HLM, are given in Supplementary Information and Extended Data Figs 4, 5, 7, 8 and 9)

Contrary to our initial hypothesis[2], the data for children with ASD show a developmental decline in eye fixation from 2 until 24 months of age (Fig. 2c, d), with average levels of ASD eye-looking that appear to begin in the normative range.

The relationship between longitudinal eye fixation and dimensional level of social-communication disability was tested using regression. As shown in Extended Data Fig. 1, steeper decline in eye fixation is associated with more severe social disability[5]: $r_{(9)} = -0.750$ (-0.27 to -0.93, 95% confidence interval), $P = 0.007$, Pearson r, 9 degrees of freedom. In an exploratory analysis, we also tested sub-sets of the available data: that is, we measured decline in eye fixation using only data collected from month 2 to 6, excluding data collected thereafter, and then using only data collected from month 2 to 9, 2 to 12, 2 to 15, and 2 to 18. The relationship between decline in eye fixation and outcome becomes a statistical trend by the subset of month 2 to 9 ($P = 0.100$), and is statistically significant thereafter. Although these analyses will benefit from replication with larger samples, they offer preliminary indication of the clinical significance of these early behaviours.

Our experimental design densely sampled the first 6 months of life in order to test the relationship between early looking behaviour and later categorical outcome. Extended Data Fig. 2a–c show raw eye-fixation data collected in the first 6 months. Eye-fixation data for both groups show significant associations with chronological age ($F_{1,114.237} = 9.94$, $P = 0.002$ for typically developing eye fixation, $F_{1,41.609} = 9.62$, $P = 0.003$ for ASD eye fixation), but the slopes of the associations are in opposite directions: increasing at +3.6% per month for typically developing (1.3 to 5.9, 95% confidence interval), and decreasing at −4.8% per month for ASD (−7.9 to −1.7, 95% confidence interval). A similar difference is observed for body fixation (Extended Data Fig. 2g–i): body fixation is declining in typically developing children but is not declining in those later diagnosed with ASD (−4.3% per month (−5.4 to −3.1) for typically developing, $F_{1,211.856} = 54.83$, $P < 0.001$; 0.3% per month for ASD (−1.2 to 1.7), $F_{1,241.320} = 0.11$, $P = 0.739$). For both regions, there are significant interactions of diagnosis by age: eyes, $F_{1,787.928} = 9.27$, $P = 0.002$; and body, $F_{1,25.557} = 5.88$, $P = 0.023$ (HLM).

As a control, we tested whether there were between-group differences in levels of looking at the video stimuli, irrespective of content region. There were no between-group differences in levels of fixation or saccading, respectively, either as a main effect of diagnosis ($F_{1,21.652} = 0.958$, $P = 0.339$; $F_{1,27.189} = 0.250$, $P = 0.621$) or as an interaction of diagnosis by age ($F_{1,20.026} = 0.880$, $P = 0.359$; $F_{1,26.430} = 0.561$, $P = 0.460$) (Extended Data Fig. 3).

Given the variability in infant looking, we measured the extent of overlap in distributions for measures of fixation in typically developing infants relative to infants later diagnosed with ASD (Fig. 3a plots individual growth curves for levels of eye fixation, and Fig. 3b plots change in eye fixation). Mean individual levels of change in fixation between 2 and 6 months show minimal overlap between groups (Fig. 3c). However, such estimates (depending as they do on the data used to build the model, with known diagnostic outcomes) are likely to be optimistic[24]; to assess bias, we performed an internal validation.

As an internal validation (Fig. 3d–f), we used leave-one-out cross-validation (LOOCV), partitioning our data into subsamples so that each infant was tested as a validation case (that is, presuming unknown diagnostic outcome) in relation to the remainder of the data set[25]. The results indicate relatively low levels of overlap between groups (Fig. 3f). The same analyses were conducted for rates-of-change in body fixation (Fig. 3g–l). Although the area under each receiver operating characteristic (ROC) curve is smaller (as expected) for the internal validations (Fig. 3f, l) compared to estimates based on known diagnostic outcomes (Fig. 3c, i), the 95% confidence intervals clearly indicate less overlap than expected by chance.

As an external validation, we used the same technique to test six male infants who were not part of the original sample. Two of the six children had reached the age of 36 months, with confirmed ASD diagnosis, and four of the children were low-risk recruits, now at least 22 months of age, with no clinical signs of ASD. In relation to the original sample's change in eye and body fixation (Fig. 3m), these six independent test cases show similar trajectories within the first 6 months (Fig. 3n). Although this validation set is small, the probability of obtaining all six of these results in the predicted direction by chance alone is $P = 0.0156$ (equal to the chance of correctly predicting the outcome, 0.5, on each of 6 occasions, 0.5^6).

As a result of observing these differences between clearly defined extremes of social functioning at outcome (ASD and typically developing), we analysed data from the remaining high-risk males. These siblings were identified clinically as either unaffected at 36 months

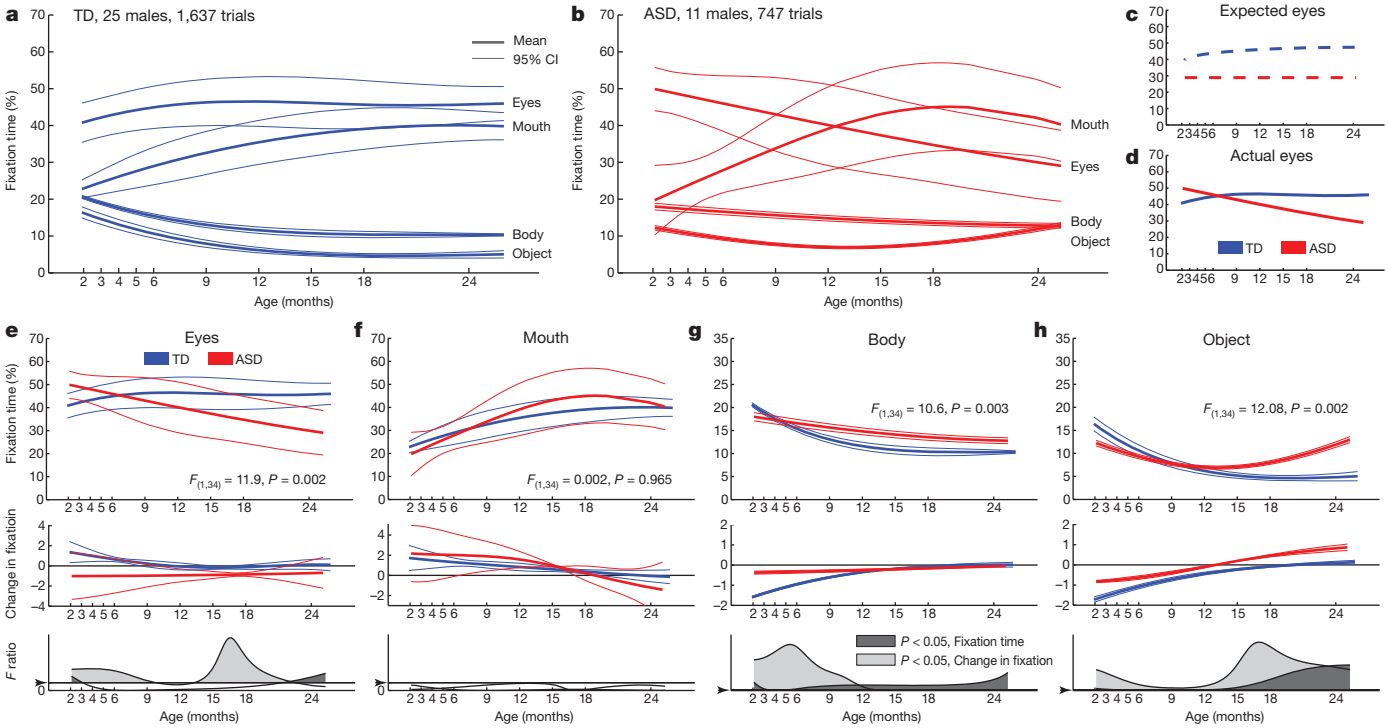

Figure 2 | Growth charts of social visual engagement for typically developing children and children diagnosed with ASD. **a**, **b**, Fixation to eyes, mouth, body and objects from 2 until 24 months in TD (**a**) and ASD (**b**) children. **c**, **d**, Contrary to a congenital reduction in preferential attention to eyes in ASD, children with ASD exhibit mean decline in eye fixation. **e**–**h**, Longitudinal change in fixation to eyes (**e**), mouth (**f**), body (**g**), and object (**h**) regions; between-group comparisons by functional ANOVA. Thick lines indicate mean growth curves, thin lines indicate 95% confidence intervals. Top panels in **e**–**h** plot per cent fixation; middle panels plot change in fixation (the first derivative, in units of % change per month); and bottom panels plot *F* value functions for between-group pointwise comparisons. Significant differences are shaded in medium grey for comparison of fixation data and light grey for comparison of change-in-fixation data, with *F* ratio critical value marked by an arrowhead on the *y* axis.

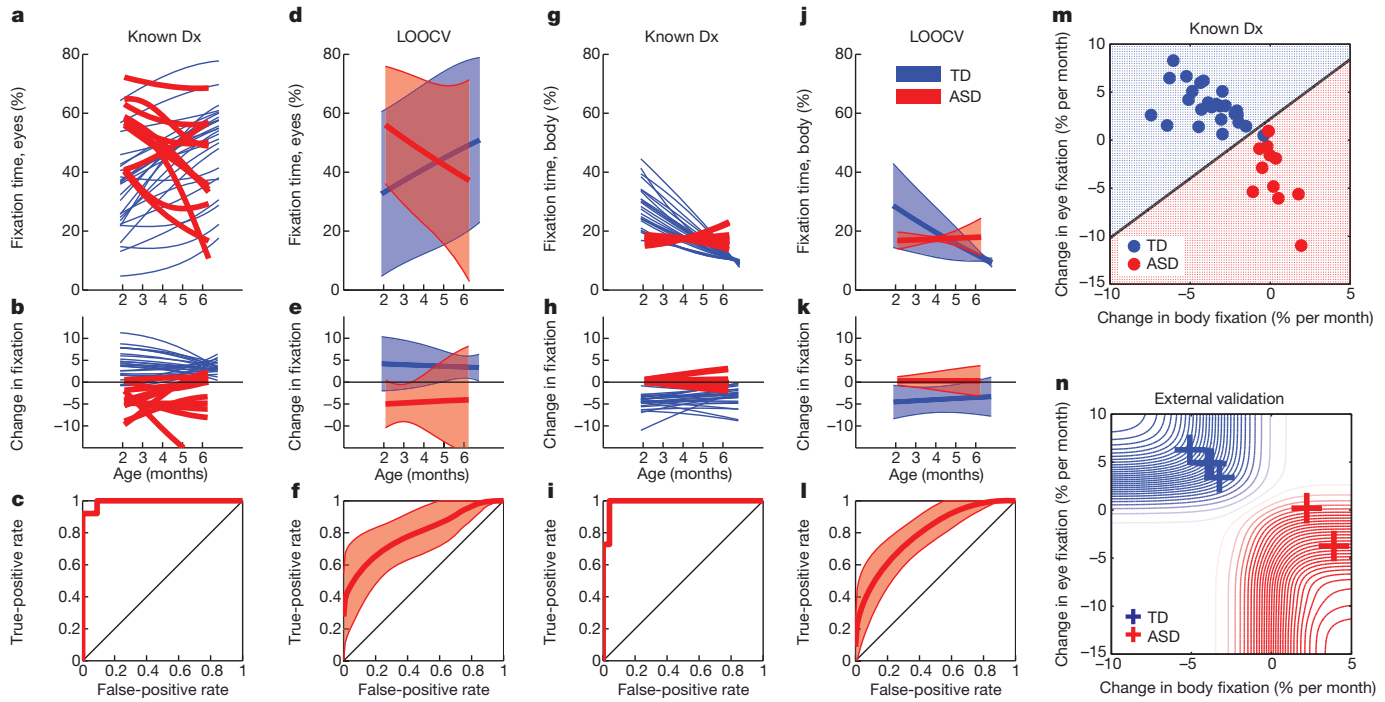

Figure 3 | Visual fixation between 2 and 6 months of age relative to diagnosis at year 3. **a**, **b**, Individual curve fits for eye-fixation data (**a**) and change-in-fixation data (**b**) for TD infants (blue) and infants later diagnosed with ASD (red). **c**, The extent of between-group overlap in distributions of change-in-fixation data with known diagnostic outcomes (Known Dx). For internal validation, each infant was tested as a validation case in relation to the remainder of the data (leave-one-out cross-validation, LOOCV). **d**, **e**, Area plots in **d** and **e** show LOOCV mean and 95% prediction intervals for individual trajectories of eye fixation (**d**) and change-in-fixation (**e**) data. **f**, The extent of between-group overlap in change-in-fixation data (mean and 95% confidence interval). **g**–**l**, The same analyses as **a**–**c** and **d**–**f**, but for body fixation, are shown in **g**–**i** and **j**–**l**. **m**, Plot of the joint distribution of change in eye and body fixation. **n**, Six male infants, not part of the original sample, were tested as an external validation.

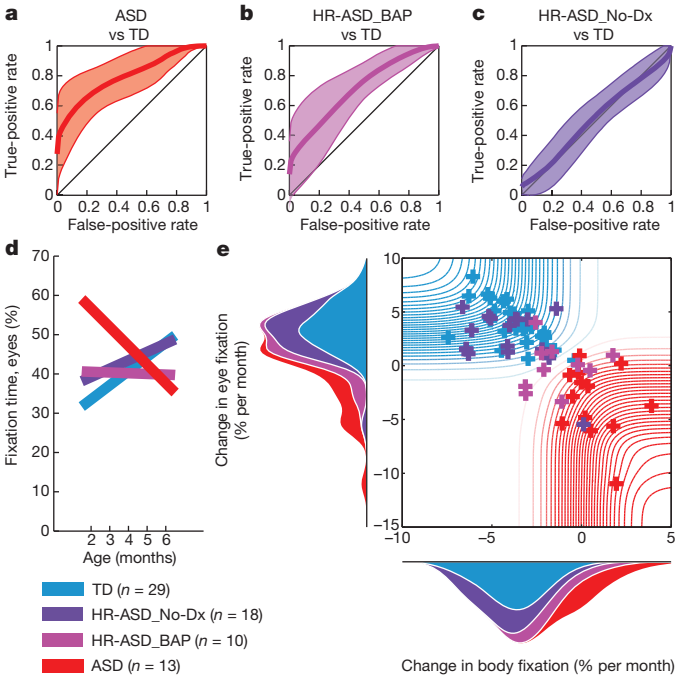

Figure 4 | Visual fixation between 2 and 6 months of age relative to outcome levels of affectedness. **a**–**c**, At 36 months, infant siblings at high risk for ASD were confirmed either as having ASD, as having subthreshold signs of ASD (HR-ASD_BAP), or as unaffected (HR-ASD_No-Dx). ROC curves in **a**, **b**, and **c** quantify overlap in measures of change in eye fixation relative to outcome (95% confidence interval by LOOCV). The behaviour of unaffected siblings overlaps with that of typically developing children (**c**), whereas the behaviour of infants later diagnosed with ASD (**a**) and that of infants with subthreshold signs (**b**) differs significantly from typical children. **d**, Eye fixation varies systematically across all outcome groups, with significant interaction of outcome by age (by HLM). **e**, Individual change in eye and body fixation for 70 infant males (29 typically developing, 25 original sample, 4 external validation; 13 ASD, 11 original sample, 2 external validation; 18 HR-ASD_No-Dx; and $N = 10$ HR-ASD_BAP). Probability density functions on ordinate and abscissa indicate distribution of measures for each outcome group.

(referred to as HR-ASD_No-Dx) or as exhibiting subthreshold signs of ASD (also called the broader autism phenotype (BAP)[26], referred to as HR-ASD_BAP). For change in eye fixation between 2 and 6 months of age, ROC curves in Fig. 4a–c quantify the overlap in measures relative to outcome (95% confidence intervals by LOOCV). The behaviour of unaffected siblings (HR-ASD_NoDx) is highly overlapping with that of typically developing children (Fig. 4c), while the behaviour of infants later diagnosed with ASD (Fig. 4a), and that of infants with subthreshold signs (Fig. 4b), clearly differs from typical controls.

We also considered these data as part of a larger continuum (Fig. 4d and Extended Data Fig. 6). Graded developmental trajectories are evident in the significant interaction of outcome (four levels) by age: $F_{3,133.006} = 6.95$, $P < 0.001$ (HLM). Typically developing children show strongly increasing eye fixation. Unaffected siblings also show increasing eye fixation. Siblings with subthreshold symptoms show neither increasing nor decreasing eye fixation, and infants later diagnosed with ASD show declining eye fixation.

In Fig. 4e, individual results are plotted dimensionally across the full spectrum of social ability to disability. The probability density functions on ordinate and abscissa indicate whole-sample distributions for change in eye and body fixation. The data show gradations from typically developing children to those diagnosed with ASD, with children with ASD showing the largest decline in eye fixation as well as the greatest increase in body fixation. Values for unaffected siblings are fully overlapping with those of typically developing children, whereas children with BAP outcomes show intermediary behaviours.

In summary, the current results indicate that the development of infants later diagnosed with ASD differs already from that of their typical peers during the period from 2 to 6 months of age. These results, although still limited in sample size, document the derailment of skills that would otherwise guide typical socialization[10,17,18], and this early divergence from normative experience suggests a means by which diverse genetic liabilities are instantiated, developmentally, into a spectrum of affectedness. Given the interdependence[9] of individual experience with brain structure and function, and with gene expression and methylation, these results suggest how a single individual's outcome will be shaped not only by initial genotypic vulnerabilities, but also by the atypical experiences that arise as a consequence of those vulnerabilities, instantiating a wide spectrum of affectedness.

In children later diagnosed with ASD, eye looking shows mean decline by at least 2 months. However, unexpectedly, those early levels of eye looking seem to begin at normative levels. This contradicts prior hypotheses of a congenital absence of social adaptive orientation[2,3,17,18] and suggests instead that some social adaptive behaviours may initially be intact in newborns later diagnosed with ASD. If confirmed in larger samples, this would offer a remarkable opportunity for treatment: predispositions that are initially intact suggest a neural foundation that may be built upon, offering far more positive possibilities than if that foundation were absent from the outset. Equally exciting, these data fit well within the framework of long-studied animal models of the neural systems subserving filial orientation and attachment[27]: they highlight a narrow period for future investigation, spanning the transition from experience-expectant to experience-dependent mechanisms[28]. A critical next step will be to measure densely sampled developmental change in gene expression and brain growth, in tandem with detailed quantification of behaviour; in short, measuring gene–brain–behaviour growth charts of infant social engagement to understand the developmental pathogenesis of social disability[29].

METHODS SUMMARY

The research protocol was approved as bearing no significant risk by the Human Investigations Committees at Yale University School of Medicine and at Emory University School of Medicine, and the data collected were used for research purposes only. All aspects of the experimental protocol were performed by personnel blinded to the diagnostic status of the children. All diagnostic measures were administered by trained clinicians blinded to results of experimental procedures. The children were shown, at each of 10 longitudinal testing points between 2 and 24 months of age, video scenes of naturalistic caregiver interaction. We measured percentage of visual fixation time to eyes, mouth, body and object regions, and these measures served as the dependent variables for longitudinal analyses. Planned confirmatory analyses measured longitudinal fixation trajectories relative to both categorical diagnostic outcomes and dimensional levels of social-communication disability. Visual scanning was measured with eye-tracking equipment (ISCAN). Analysis of eye movements and coding of fixation data were performed with software written in MATLAB. Additional details on participants, experimental procedures, data acquisition and analysis are provided in Methods and in Supplementary Information.

Online Content Any additional Methods, Extended Data display items and Source Data are available in the online version of the paper; references unique to these sections appear only in the online paper.

Received 28 January; accepted 24 September 2013.
Published online 6 November 2013.

1. Grice, S. J. *et al.* Neural correlates of eye-gaze detection in young children with autism. *Cortex* **41,** 342–353 (2005).
2. Jones, W., Carr, K. & Klin, A. Absence of preferential looking to the eyes of approaching adults predicts level of social disability in 2-year-olds with autism spectrum disorder. *Arch. Gen. Psychiatry* **65,** 946–954 (2008).
3. Kanner, L. Autistic disturbances of affective contact. *Nerv. Child* **2,** 217–250 (1943).
4. Volkmar, F. R., Lord, C., Bailey, A., Schultz, R. T. & Klin, A. Autism and pervasive developmental disorders. *J. Child Psychol. Psychiatry* **45,** 135–170 (2004).
5. Lord, C., Rutter, M., DiLavore, P. & Risi, S. *Autism Diagnostic Observation Schedule* 2nd edn (Western Psychological Services, 2008).

6. Centers for Disease Control and Prevention. Prevalence of autism spectrum disorders — Autism and Developmental Disabilities Monitoring Network, 14 Sites, United States, 2008. *MMWR Surveillance Summaries* **61,** 1–19 (2012).
7. Constantino, J. N. *et al.* Autism recurrence in half siblings: strong support for genetic mechanisms of transmission in ASD. *Mol. Psychiatry* **18,** 137–138 (2013).
8. State, M. W. & Sestan, N. Neuroscience: the emerging biology of autism spectrum disorders. *Science* **337,** 1301–1303 (2012).
9. Oyama, S. *The Ontogeny of Information: Developmental Systems and Evolution* 2nd edn (Duke Univ. Press, 2000).
10. Jones, W. & Klin, A. Heterogeneity and homogeneity across the autism spectrum: the role of development. *J. Am. Acad. Child Adolesc. Psychiatry* **48,** 471–473 (2009).
11. DeCasper, A. J. & Fifer, W. P. Of human bonding: newborns prefer their mothers' voices. *Science* **208,** 1174–1176 (1980).
12. Haith, M. M., Bergman, T. & Moore, M. J. Eye contact and face scanning in early infancy. *Science* **198,** 853–855 (1977).
13. Johnson, M. H. Subcortical face processing. *Nature Rev. Neurosci.* **6,** 766–774 (2005).
14. Simion, F., Regolin, L. & Bulf, H. A predisposition for biological motion in the newborn baby. *Proc. Natl Acad. Sci. USA* **105,** 809–813 (2008).
15. Johnson, M. H. Functional brain development in humans. *Nature Rev. Neurosci.* **2,** 475–483 (2001).
16. Rosa Salva, O., Farroni, T., Regolin, L., Vallortigara, G. & Johnson, M. H. The evolution of social orienting: evidence from chicks (*Gallus gallus*) and human newborns. *PLoS ONE* **6,** e18802 (2011).
17. Klin, A., Jones, W., Schultz, R. T. & Volkmar, F. The enactive mind — from actions to cognition: lessons from autism. *Phil. Trans. R. Soc. B* **358,** 345–360 (2003).
18. Klin, A., Lin, D. J., Gorrindo, P., Ramsay, G. & Jones, W. Two-year-olds with autism fail to orient towards human biological motion but attend instead to non-social, physical contingencies. *Nature* **459,** 257–261 (2009).
19. Ozonoff, S. *et al.* Recurrence risk for autism spectrum disorders: a Baby Siblings Research Consortium study. *Pediatrics* **128,** e488–e495 (2011).
20. Chawarska, K., Klin, A., Paul, R. & Volkmar, F. R. Autism spectrum disorders in the second year: stability and change in syndrome expression. *J. Child Psychol. Psychiatry* **48,** 128–138 (2007).
21. Ramsay, J. O. & Silverman, B. W. *Functional Data Analysis* 2nd edn (Springer-Verlag, 2006).
22. Yao, F., Müller, H. G. & Wang, J. L. Functional data analysis for sparse longitudinal data. *J. Am. Stat. Assoc.* **100,** 577–590 (2005).
23. Singer, J. D. & Willett, J. B. *Applied Longitudinal Data Analysis* (Oxford Univ. Press, New York, 2003).
24. Mosteller, F. & Tukey, J. W. *Data Analysis and Regression* 37 (Addison-Wesley, 1977).
25. Stone, M. Cross-validatory choice and assessment of statistical predictions. *J. R. Stat. Soc. B* **36,** 111–147 (1974).
26. Steer, C. D., Golding, J. & Bolton, P. F. Traits contributing to the autistic spectrum. *PLoS ONE* **5,** e12633 (2010).
27. Horn, G., Nicol, A. U. & Brown, M. W. Tracking memory's trace. *Proc. Natl Acad. Sci. USA* **98,** 5282–5287 (2001).
28. Johnson, M. H. & Karmiloff-Smith, A. In *Theories of Infant Development* (eds Bremner, G. & Slater, A.) 121–141 (Blackwell, 2004).
29. Abrahams, B. S. & Geschwind, D. H. Advances in autism genetics: on the threshold of a new neurobiology. *Nature Rev. Genet.* **9,** 341–355 (2008).

Supplementary Information is available in the online version of the paper.

Acknowledgements This work was supported by grants from the Simons Foundation and the National Institute of Mental Health (R01 MH083727). Additional support was provided by the Marcus Foundation, the Whitehead Foundation, and the Georgia Research Alliance. We wish to thank the families and children for their time and participation. We also wish to thank S. Habayeb, S. Glazer, M. Ly, T. Tsang, J. Jones, A. Trubanova, J. Borjon, J. Moriuchi, K. Rice, J. Northrup, L. Edwards, J. Xu, S. Shultz, A. Krasno, C. Zampella, K. Knoch, D. Lin, K. Carr and A. Blank for their assistance in data collection and processing; P. Lewis, J. Paredes, P. Gorrindo and M. Ackerman for assistance in designing and building laboratory hardware and software; G. Ramsay and C. McCracken for discussions of data analysis and statistics; I. Zilber, A. Margolis, D. Blum, M. Dye, D. Simeone, A. Smith and K. O'Loughlin for project supervision, coordination, and data collection; T. Babitz for administrative support; and K. Chawarska, C. Saulnier, K. Bearss, S. Macari, R. Paul, A. Carney, T. Goldsmith, A. Steiner, G. Gengoux, D. Goudreau, E. Loring, J. McGrath and A. Gupta for their contributions to the clinical characterization of the samples.

Author Contributions W.J. and A.K. developed the initial idea and design of the study, interpreted data, wrote the final manuscript, had full access to all of the data in the study and take responsibility for the integrity of the data and the accuracy of the data analysis. W.J. and A.K. performed final revision of the manuscript for content. A.K. supervised participant characterization. W.J. supervised technological developments and technical aspects of experimental procedure, data acquisition and analysis.

Author Information Reprints and permissions information is available at www.nature.com/reprints. The authors declare no competing financial interests. Readers are welcome to comment on the online version of the paper. Correspondence and requests for materials should be addressed to W.J. (warren.jones@emory.edu) or A.K. (ami.klin@emory.edu).

METHODS

The research protocol was approved as bearing no significant risk by the Human Investigations Committees at Yale University School of Medicine and at Emory University School of Medicine, and the data collected were used for research purposes only. All aspects of the experimental protocol were performed by personnel blinded to the diagnostic status of the children. All diagnostic measures were administered by trained clinicians blind to results of experimental procedures. The children were shown, at each of 10 longitudinal testing points between 2 and 24 months of age, video scenes of naturalistic caregiver interaction. We measured percentage of visual fixation time to eyes, mouth, body and object regions, and these measures served as the dependent variables for longitudinal analyses. Planned confirmatory analyses measured longitudinal fixation trajectories relative to both categorical diagnostic outcomes and dimensional levels of social-communicative disability. Visual scanning was measured with eye-tracking equipment (ISCAN). Analysis of eye movements and coding of fixation data were performed with software written in MATLAB. Additional details on participants, experimental procedures, data acquisition and analysis are provided in Methods and in Supplementary Information.

Stimuli. Children were shown video scenes of a female actor looking directly into the camera and playing the part of a caregiver: entreating the viewing toddler by engaging in childhood games (for example, playing pat-a-cake) (Fig. 1a, b; also described in ref. 2). The actors were filmed in naturalistic settings that emulated the real-world environment of a child's room, with pictures, shelves of toys, and stuffed animals. We used naturalistic stimuli (for example, dynamic rather than static stimuli, and realistic rather than abstracted or reductive scenes) in light of past research indicating that older children with ASD exhibit large discrepancies between their actual adaptive behaviour skills in the real world relative to their cognitive potential in more structured situations[30], larger between-group effect sizes for face-processing deficits with dynamic relative to static stimuli[31], and marked difficulties when attempting to generalize skills from structured, rote environments (in which the skills were initially learned) to environments that are open-ended and rapidly changing[4]. At each data-collection session, videos were drawn in pseudo-random order from a pool of 35 total. Both the 'caregiver' video stimuli analysed here (35 videos), as well as videos of infant and toddler interaction ('peer-play' videos, as described in ref. 32, for another set of experiments not yet analysed) were presented. Video stimuli were presented in pseudo-random order. There were no between-group differences in duration of data collected per child, either in total ($t_{34} = 0.685$, $P = 0.498$) or specifically for the caregiver stimuli ($t_{34} = 0.205$, $P = 0.839$). Successful data collection was achieved in 80.2% of all testing sessions; failed data collection sessions occurred as the result of an infant falling asleep, crying, or becoming too fussy to watch the videos. Reasons for failure were recorded in data collection reports for each session and maintained in a database; no systematic difference in reasons for failure could be discerned between the two groups. At each data collection session, approximately 30% of the videos shown to a child were novel, whereas the remaining 70% were repeated from previous sessions (from both the immediately preceding session as well as from any prior session beginning at month 2 onwards). This balanced the need for repeated measures to the same stimulus video with the need for novelty. To test for learning effects of repeated presentations, we compared end-stage results at 24 months in this longitudinal sample with previous results in a cross-sectional sample at that age (males from ref. 2): tested by 2×2 between-subjects factorial ANOVA, there was no main effect of cohort, longitudinal versus cross-sectional ($F_{1,57} = 0.052$, $P = 0.820$), but there was a significant main effect of diagnosis (ASD versus typically developing, $F_{1,57} = 6.29$, $P = 0.015$).

Caregiver videos were presented as full-screen audiovisual stimuli on a 20-inch computer monitor (refresh rate of 60 Hz noninterlaced); in 32-bit colour; at 640×480 pixels in resolution; at 30 frames per s; with mono-channel audio sampled at 44.1 kHz. Stimuli were sound and luminosity equalized, and were piloted before the start of study in order to optimize engagement for typical infant and toddler viewers. Regions of interest (eye, mouth, body and object) were bitmapped in all frames of video (Fig. 1c). Average sizes of the regions-of-interest are given in Extended Data Table 1c.

Experimental setting and equipment. Two settings for eye-tracking data collection were used in this study. One eye-tracking laboratory was optimized for infants between the ages of 2 and 6 months, and a second setting was optimized for infants and toddlers from 9 to 36 months. The primary distinction between the two settings was the use of a reclined bassinet for younger infants versus the use of a car seat for older infants and toddlers. The eye-tracking data-collection hardware and software were identical in both settings, and all aspects of automated stimuli presentation, data collection and analysis were also identical; these have previously been described in ref. 2. To obtain optimal eye imaging with infants in the reclined bassinet, eye-tracking cameras and an infrared light source were concealed within a teleprompter. In the toddler laboratory, eye-tracking cameras were mounted beneath a computer display monitor. The display monitor was mounted flush within a wall panel. In both laboratories, eye tracking was accomplished by a video-based, dark pupil/corneal reflection technique with hardware and software created by ISCAN, with data collected at 60 Hz. In both laboratories, audio was played through a set of concealed speakers. Infants were placed in a modified travel bassinet, mounted on a table that was raised and lowered at the beginning of each session to standardize the positioning of the infant's eyes relative to the display monitor. In the toddler laboratory, children were seated in a car seat in front of the computer screen on which the videos were presented. As in the infant laboratory, the car seat was raised and lowered so as to standardize the position of each child's eyes relative to the display monitor.

Experimental protocol. Infants and toddlers were accompanied at all times by a parent or primary caregiver. To begin the experimental session, the participant (infant or toddler) and caregiver entered the laboratory room while a popular children's entertainment video played on the display monitor. The child was buckled into the bassinet or car seat. Eye position relative to display monitor was then standardized for each child by adjusting the seat or bassinet location. Viewers' eyes were 28 inches (71.12 cm) from the display monitor, which subtended an approximately $24^\circ \times 32^\circ$ portion of each viewer's visual field. Lights in the room were dimmed so that only content presented on the display monitor could be easily seen. During testing, both experimenter and parent were out of view from the child but were able to monitor the child at all times by means of an eye-tracking camera and by a second video camera that filmed a full-body image of the child.

Visual-fixation patterns were measured with eye-tracking hardware (ISCAN). To begin the process of data collection, after the child was comfortably watching the children's video, calibration targets were presented onscreen by the experimenter. This was done using software that paused the playing video and presented a calibration target on an otherwise blank background. A five-point calibration scheme was used, presenting spinning and/or flashing points of light as well as cartoon animations, ranging in size from 1° to 1.5° of visual angle, all with accompanying sounds. For the infants, calibration stimuli began as large targets, $\geq 10^\circ$ in horizontal and vertical dimensions, which then shrank through animation to their final size of 1° to 1.5° of visual angle. The calibration routine was followed by verification of calibration in which more animations were presented at five on-screen locations. Throughout the remainder of the testing session, animated targets (as used in the calibration process) were shown between experimental videos to measure drift in calibration accuracy. In this way, accuracy of the eye-tracking data was verified before beginning experimental trials and was then repeatedly checked between video segments as the testing continued. In the case that drift exceeded 3°, data collection was stopped and recalibration was carried out before further videos were presented. For additional details and measures of calibration accuracy, please see Supplementary Information and Extended Data Fig. 8.

Analysis of eye movements. Analysis of eye movements and coding of fixation data were performed with software written in MATLAB (MathWorks). The first phase of analysis was an automated identification of non-fixation data, comprising blinks, saccades and fixations directed away from the presentation screen. Saccades were identified by eye velocity using a threshold of 30° per s (ref. 33). We tested the velocity threshold with the 60-Hz eye-tracking system described above and, separately, with an eye-tracking system collecting data at 500 Hz (SensoMotoric Instruments GmbH). In both cases saccades were identified with equivalent reliability as compared with both hand coding of the raw eye-position data and with high-speed video of the child's eyes. Blinks were identified as described in ref. 32. Off-screen fixations (when a participant looked away from the video) were identified by fixation coordinates beyond the stimuli presentation screen.

Eye movements identified as fixations were coded into four regions of interest that were defined within each frame of all video stimuli: eyes, mouth, body (neck, shoulders and contours around eyes and mouth, such as hair) and objects (surrounding inanimate stimuli) (Fig. 1c). The regions of interest were hand traced for all frames of the video and were then stored as binary bitmaps (through software written in MATLAB). Automated coding of fixation time to each region of interest then consisted of a numerical comparison of each child's coordinate fixation data with the bitmapped regions of interest.

Longitudinal data analyses. To examine the longitudinal development of social visual attention, for individual participants and across both ASD and typically developing groups, we used functional data analysis (FDA)[21] and principal analysis by conditional expectation (PACE)[22,34–36] (Fig. 1d, e for example individual fits, and Fig. 2 for group results; also Extended Data Fig. 7). Although we focused on FDA and PACE in order to overcome limitations inherent to cross-sectional analyses, as well as some limitations of traditional growth-curve analyses, we repeated all our analyses using hierarchical linear modelling (HLM) (Extended Data Figs 4, 5 and 6 and Extended Data Table 1b). Although the two methods produced the same pattern of significant between-group differences (described in

main text and in Supplementary Information), we favour the FDA approach because traditional growth-curve analyses can be confounded by individual differences in developmental timescale, and also because traditional growth curve analyses often require correct assumption of an underlying parametric or semi-parametric model (rather than allowing this to be determined in a data-driven fashion[37]). In contrast, FDA methods determine curve shape empirically[22,35] and model statistical variation in both time scale as well as amplitude[34,36]. The PACE method of FDA is also designed specifically to overcome a common problem for longitudinal studies: non-uniform sampling particularly in the case of missing values[22,35]. PACE characterizes statistical ensembles of irregularly sampled longitudinal data in terms of entire curve shapes on the basis of conditional expectation. This maximizes the ability to detect patterns of correlation across trajectories and minimizes the impact of data sampled at discrete intervals with varying number of measurements per participant[36]. This approach notably improves the detection of common features in trajectory shape.

As noted above, as a methodological comparison to FDA, we also analysed the data using hierarchical linear modelling[23]. The presence of linear and curvilinear (quadratic and cubic) patterns was assessed for fixation relative to age using the following model:

$$\text{fixation}_{ij} = \text{intercept}_j + \text{d}_{ij} + B_{1j}(\text{age}_{\text{ij}}) + B_{2j}(\text{age}_{ij})^2 + B_{3j}(\text{age}_{ij})^3 + e_{ij}$$

where d_{ij} represents the normally distributed random effect modelling within-subject dependence (i) by group (j); e_{ij} represents the normally distributed residual error; and the B_1, B_2, and B_3 coefficients indicate how fixation levels change with age and by group. Initial evaluation of the data indicated an inverse relationship between body fixation and age, and was therefore also assessed with the following model:

$$\text{body fixation}_{ij} = d_i + \text{intercept}_j + (B_{1j}/\text{age}_{ij}) + e_{ij}$$

In all cases, the intercept and B terms were modelled as fixed effects but were allowed to vary by group. Degrees of freedom were calculated by the Satterthwaite method (equal variances not assumed). Positively skewed data (for example, body- and object-fixation trials) were log-transformed; plots show untransformed data. *F* tests and log-likelihood ratios were used to determine whether a linear, quadratic, cubic or inverse relationship best described the data. Growth curves from hierarchical linear modelling are plotted in Extended Data Figs 4 and 5, and the regression parameters for eyes, mouth, body and object are given in Extended Data Table 1a.

Throughout our analyses, PACE parameters were selected by generalized cross-validation[22]. Mean fixation curves from Fig. 2 , together with the effects of adding or subtracting principal component functions (following the convention of ref. 21), smoothing kernel bandwidths, and fractions of variance explained per principal component can be found in Extended Data Fig. 7 and Extended Data Table 1b). The Akaike Information Criterion, with likelihood of measurements conditional on estimated random coefficients, was applied for selecting the number of principal components[22]. Derivatives were computed by the PACE-QUO method[35].

30. Klin, A. *et al.* Social and communication abilities and disabilities in higher functioning individuals with autism spectrum disorders. *J. Autism Dev. Disord.* **37,** 748–759 (2007).
31. Speer, L. L., Cook, A. E., McMahon, W. M. & Clark, E. Face processing in children with autism: effects of stimulus contents and type. *Autism* **11,** 265–277 (2007).
32. Shultz, S., Klin, A. & Jones, W. Inhibition of eye blinking reveals subjective perceptions of stimulus salience. *Proc. Natl Acad. Sci. USA* **108,** 21270–21275 (2011).
33. Leigh, R. J. & Zee, D. S. *The Neurology of Eye Movements* 3rd edn (Oxford Univ. Press, 1999).
34. Hall, P., Müller, H.-G. & Yao, F. Estimation of functional derivatives. *Ann. Stat.* **37,** 3307–3329 (2009).
35. Liu, B. & Müller, H. G. Estimating derivatives for samples of sparsely observed functions, with application to online auction dynamics. *J. Am. Stat. Assoc.* **104,** 704–717 (2009).
36. Tang, R. & Müller, H.-G. Pairwise curve synchronization for functional data. *Biometrika* **95,** 875–889 (2008).
37. Burchinal, M., Nelson, L. & Poe, M. In *Best Practices in Quantitative Methods for Developmentalists* (eds McCartney, K.,Burchinal, M. & Bub, K.) *Monogr. Soc. Res. Child Dev.* **71,** 65–87 (2006).

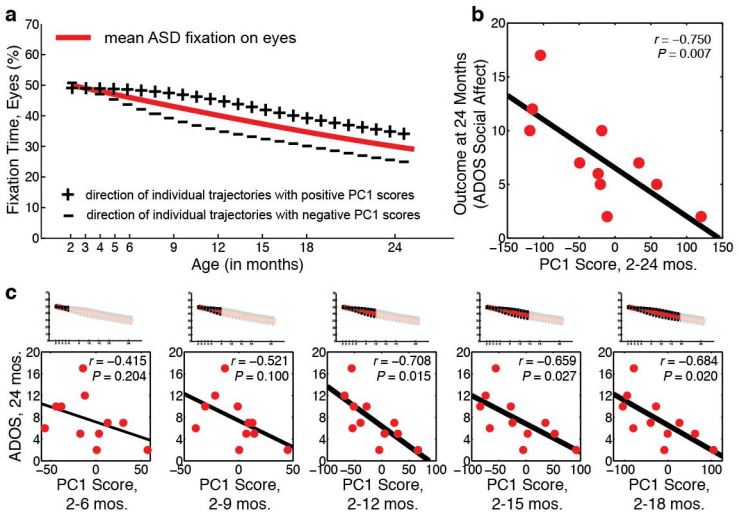

Extended Data Figure 1 | In infants later diagnosed with ASD, decline in eye fixation during the first 2 years is significantly associated with outcome levels of symptom severity. Functional principal component analysis (FPCA) was used to extract growth curve components explaining variance in trajectory shape about the population mean. **a**, Population mean for fixation to eyes in children with ASD (red line) plotted with lines indicating direction of individual trajectories having positive principal component one (PC1) scores (line marked by plus signs) or negative PC1 scores (line marked by minus signs). **b**, Outcome levels of social disability (as measured by ADOS Social Affect) as a function of decline in eye fixation (measured as eyes PC1 score). **c**, Outcome levels of social disability as a function of decline in eye fixation using subsets of the longitudinal data (that is, measuring decline in eye fixation using only data collected from month 2 to 6, excluding data thereafter; then from month 2 to 9, 2 to 12, 2 to 15, and 2 to 18). Decline in eye fixation predicts future outcome at trend levels by the developmental period from 2 to 9 months ($P = 0.100$), and is statistically significant thereafter.

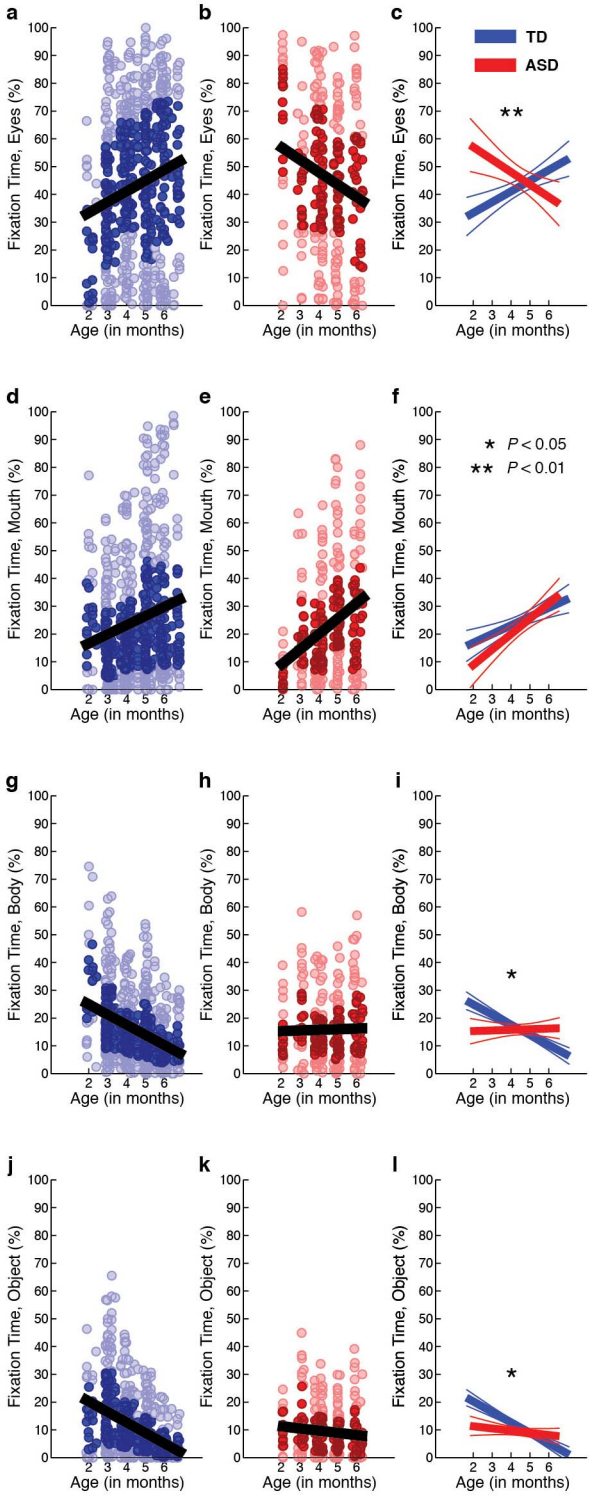

Extended Data Figure 2 | Developmental differences in visual fixation between 2 and 6 months of age. **a–l**, Raw data for eyes fixation (**a–c**), mouth fixation (**d–f**), body fixation (**g–i**), and object fixation (**j–l**) between 2 and 6 months for typically developing infants (in blue) and infants later diagnosed with autism spectrum disorders (in red). Darkly shaded data markers indicate the interquartile range (spanning 25th to 75th percentiles). Data show significant associations with chronological age, but the slopes of the associations differ for ASD and TD outcome groups, with significant interactions of diagnosis by age for eyes, $F_{1,787.928} = 9.27$, $P = 0.002$; for body, $F_{1,25.557} = 5.88$, $P = 0.023$; and for object, $F_{1,21.947} = 5.24$, $P = 0.032$; but not for mouth, $F_{1,47.298} = 0.019$, $P = 0.89$. Analyses by HLM. Plots in **c**, **f**, **i** and **l** show mean trend lines and 95% confidence intervals.

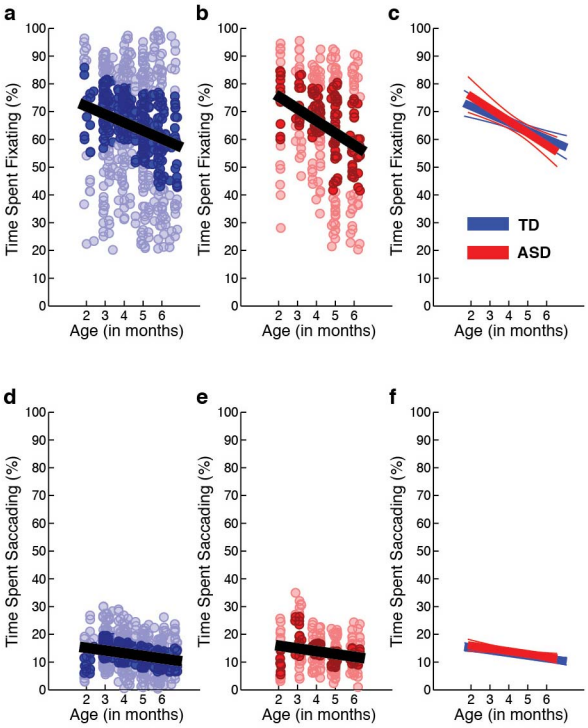

Extended Data Figure 3 | Percentage of total time spent fixating and saccading between 2 and 6 months of age. **a**–**f**, Raw data for percentage of total time spent fixating (**a**–**c**) and time spent saccading (**d**–**f**) between 2 and 6 months for typically developing infants (in blue) and infants later diagnosed with autism spectrum disorders (in red). Darkly shaded data markers indicate the interquartile range (spanning 25th to 75th percentiles). Data show significant associations with chronological age, but the slopes of the associations do not differ for ASD and TD outcome groups, $F_{1,20.026} = 0.88$, $P = 0.359$ for time spent fixating; and $F_{1,26.430} = 0.56$, $P = 0.460$ for time spent saccading. Analyses by HLM. Plots in **c** and **f** show mean trend lines and 95% confidence intervals.

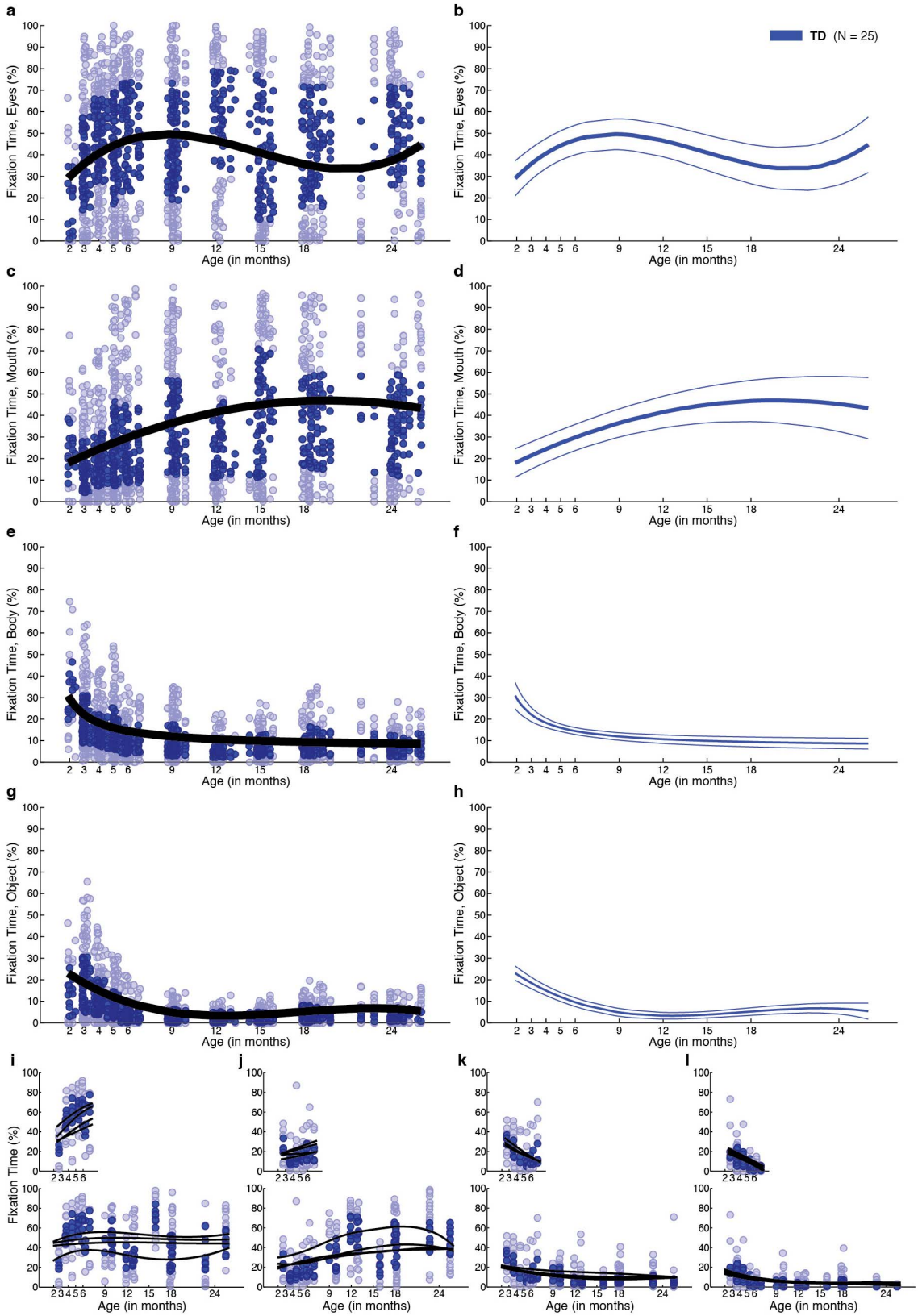

Extended Data Figure 4 | Developmental change in visual fixation between 2 and 24 months of age in typically developing children. **a**, **c**, **e**, **g**, Raw data for eyes fixation (**a**), mouth fixation (**c**), body fixation (**e**) and object fixation (**g**) between 2 and 24 months for typically developing children. Black lines indicates mean growth curves via hierarchical linear modelling (HLM). **b**, **d**, **f**, **h**, Mean fixation curves with 95% confidence intervals for eyes fixation (**b**), mouth fixation (**d**), body fixation (**f**) and object fixation (**h**) between 2 and 24 months for typically developing children. **i**–**l** Raw data for eyes fixation (**i**), mouth fixation (**j**), body fixation (**k**) and object fixation (**l**) between 2 and 6 months (top row), and 2 and 24 months (bottom row), together with individual fits, in black, for typically developing external validation sample ($n = 4$). Throughout all plots, darkly shaded data markers indicate the interquartile range (spanning 25th to 75th percentiles).

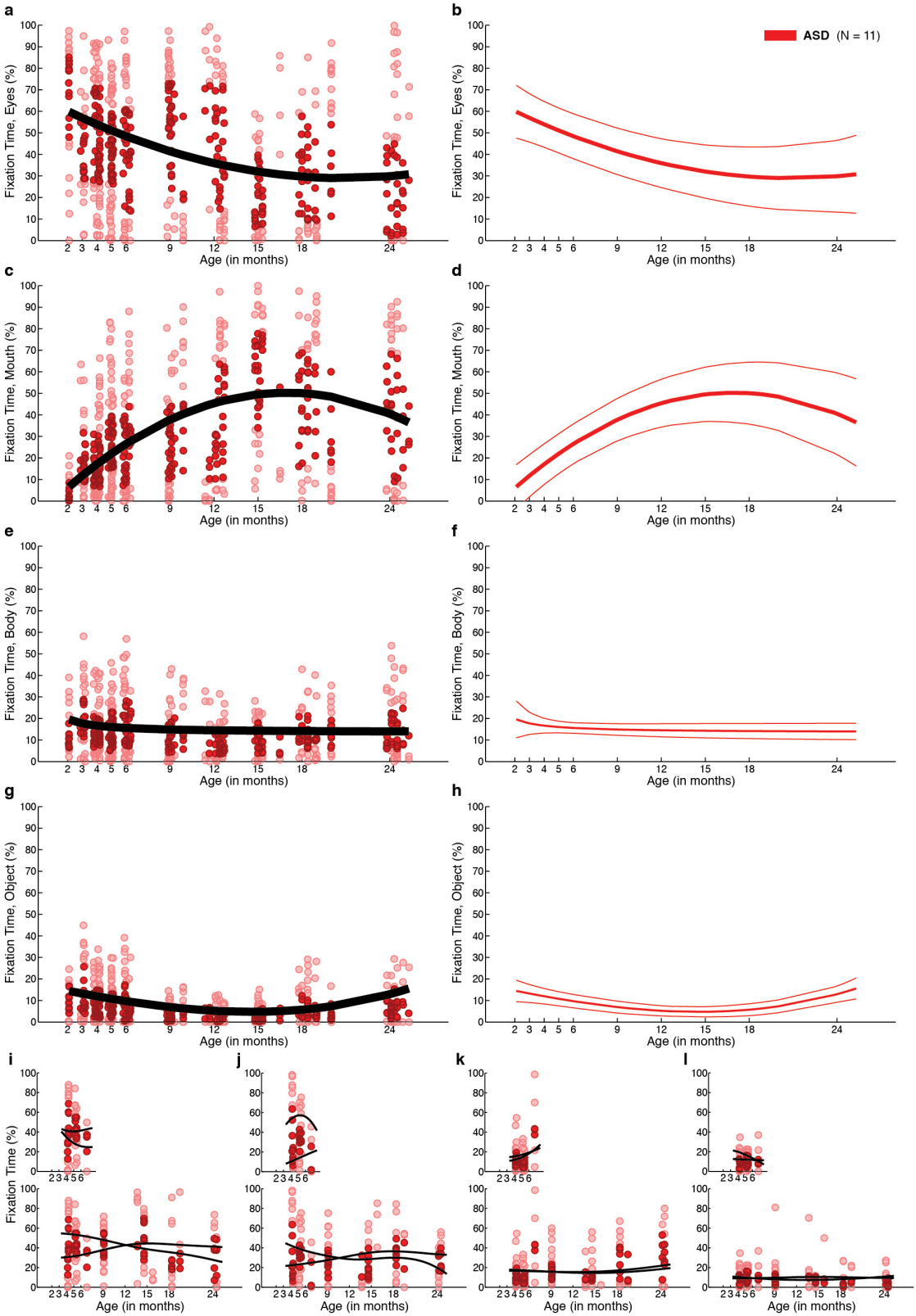

Extended Data Figure 5 | Developmental change in visual fixation between 2 and 24 months of age in children with ASD. **a**, **c**, **e**, **g**, Raw data for eyes fixation (**a**), mouth fixation (**c**), body fixation (**e**) and object fixation (**g**) between 2 and 24 months for children with ASD. Black lines indicates mean growth curves via hierarchical linear modelling (HLM). **b**, **d**, **f**, **h**, Mean fixation curves with 95% confidence intervals for eyes fixation (**b**), mouth fixation (**d**), body fixation (**f**) and object fixation (**h**) between 2 and 24 months for children with ASD. **i**–**l** Raw data for eyes fixation (**i**), mouth fixation (**j**), body fixation (**k**) and object fixation (**l**) between 2 and 6 months (top row), and 2 and 24 months (bottom row), together with individual fits, in black, for external validation sample of children infants later diagnosed with ASD ($n = 2$). Throughout all plots, darkly shaded data markers indicate the interquartile range (spanning 25th to 75th percentiles).

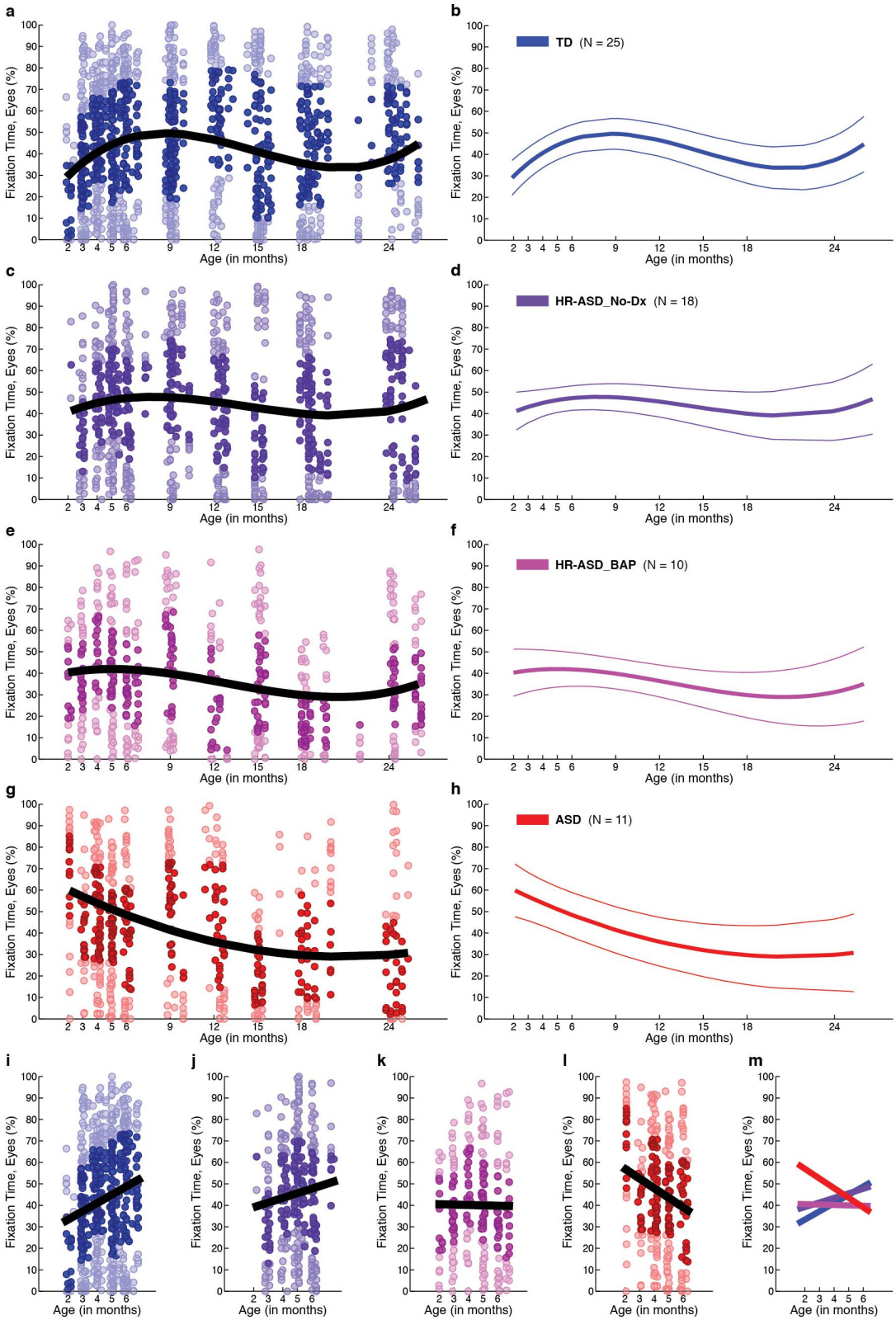

Extended Data Figure 6 | Developmental change in visual fixation on the eyes relative to outcome levels of affectedness. **a**–**m**, Per cent fixation on eyes for typically developing infants (**a**), infants at high-risk for ASD who showed no evidence of ASD at 36 months (**c**) (HR-ASD_No-Dx), infants at high-risk for ASD who showed some subthreshold signs of the broader autism phenotype at 36 months but did not meet clinical best estimate diagnosis of ASD (**e**) (HR-ASD_BAP), and infants diagnosed with ASD at 36 months (**g**). External validation participants not included (compare to Fig. 4). Darkly shaded data markers indicate the interquartile range (spanning 25th to 75th percentiles). Black lines indicate mean growth curves from hierarchical linear modelling (HLM). Plots in **b**, **d**, **f** and **h** show mean fixation curves with 95% confidence intervals. Plots **i**–**l** highlight the first 6 months of life in each group, and **m** plots the relationship across groups.

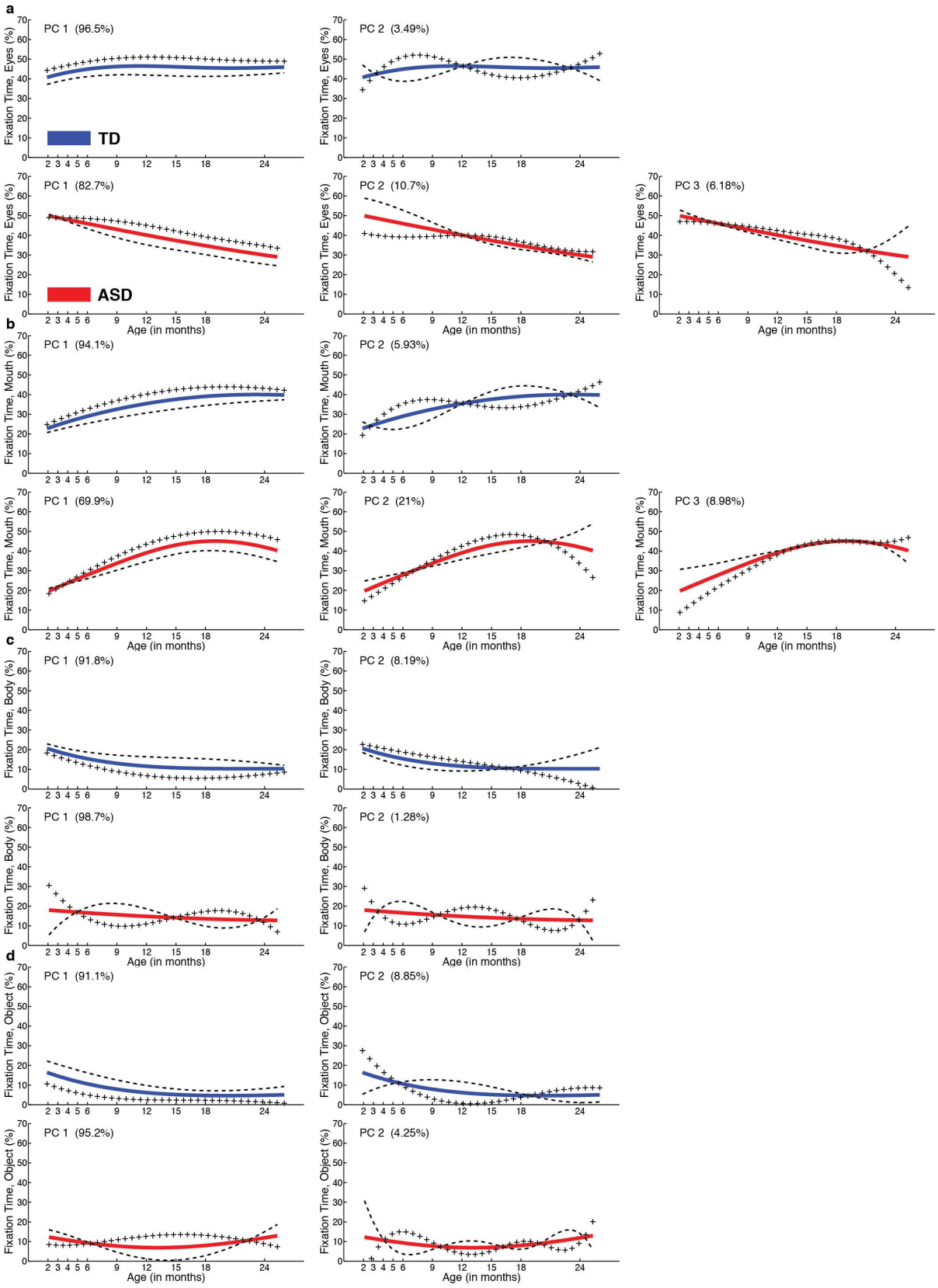

Extended Data Figure 7 | Mean fixation curves by PACE and FDA with the effects of adding or subtracting principal component functions (following the convention of Ramsay and Silverman, ref. 21). **a**–**d**, Fixation for typically developing infants (in blue) and infants with ASD (in red). **a**, Eye fixation. **b**, Mouth fixation. **c**, Body fixation. **d**, Object fixation. For each region and each group, the number of plots is dictated by number of principal component (PC) functions. The number of PC functions was determined by the Akaike Information Criterion. The fraction of variance explained (FVE) is given in parentheses in the upper left corner of each plot. The mean functions in each case match those plotted in Fig. 2. In all parts, + signs indicate the addition of PC functions; − signs indicate the subtraction of PC functions.

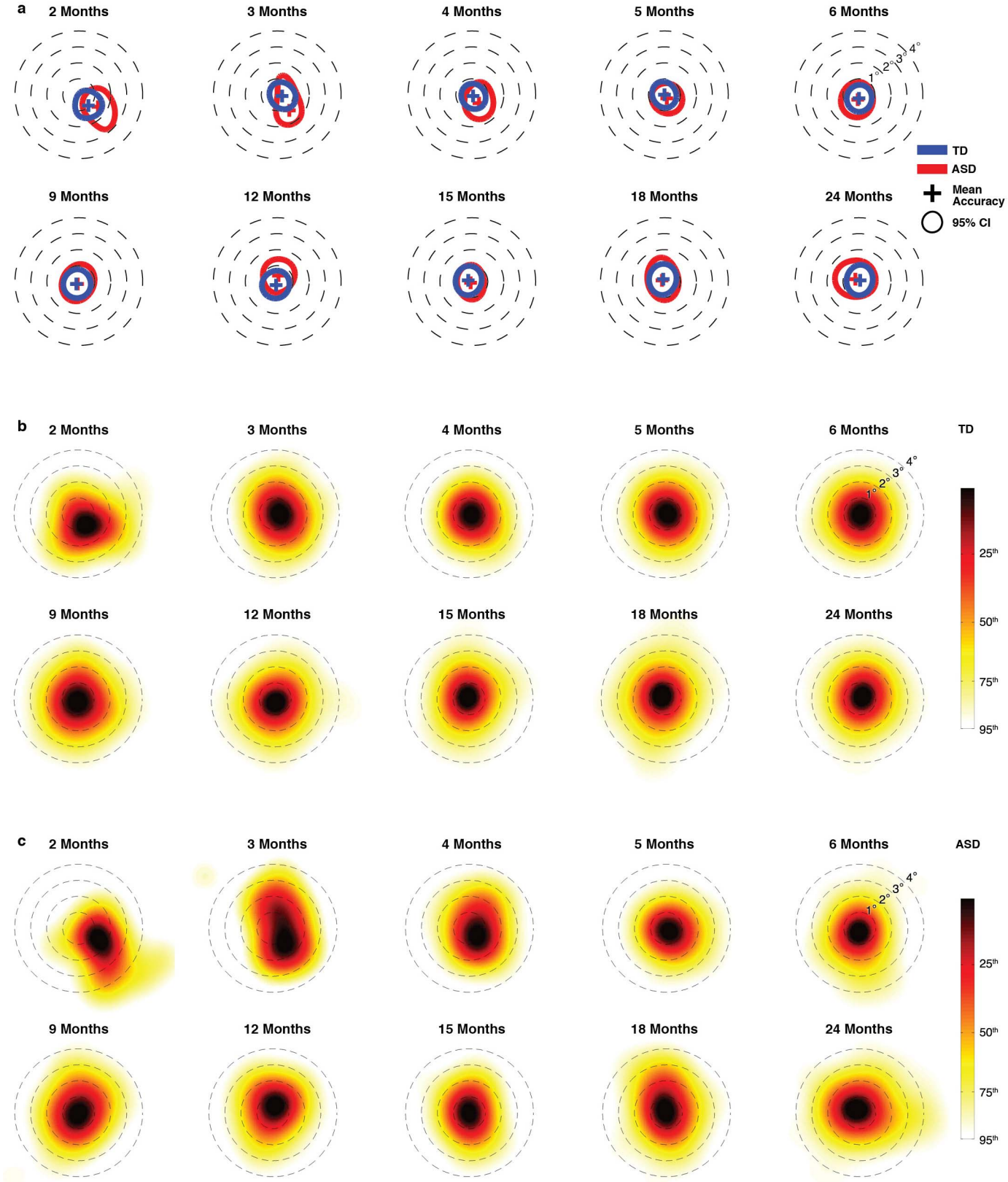

Extended Data Figure 8 | Calibration accuracy from 2 until 24 months of life in TD children and in children diagnosed with an ASD. a–c, In plots in **a**, the cross marks the location of mean calibration accuracy, and the annulus marks the 95% confidence interval (CI). In **b**, kernel density estimates plot the distribution of fixation locations relative to fixation targets for TD children. In **c**, kernel density estimates plot the distribution of fixation locations relative to fixation targets for children diagnosed with an ASD. Smoothing bandwidth for kernel density estimates was equal to 1°. Targets for testing calibration accuracy consisted of spinning and/or flashing points of light and cartoon animations, ranging in size from 1° to 1.5° of visual angle, presented on an otherwise blank screen, all with accompanying sounds.

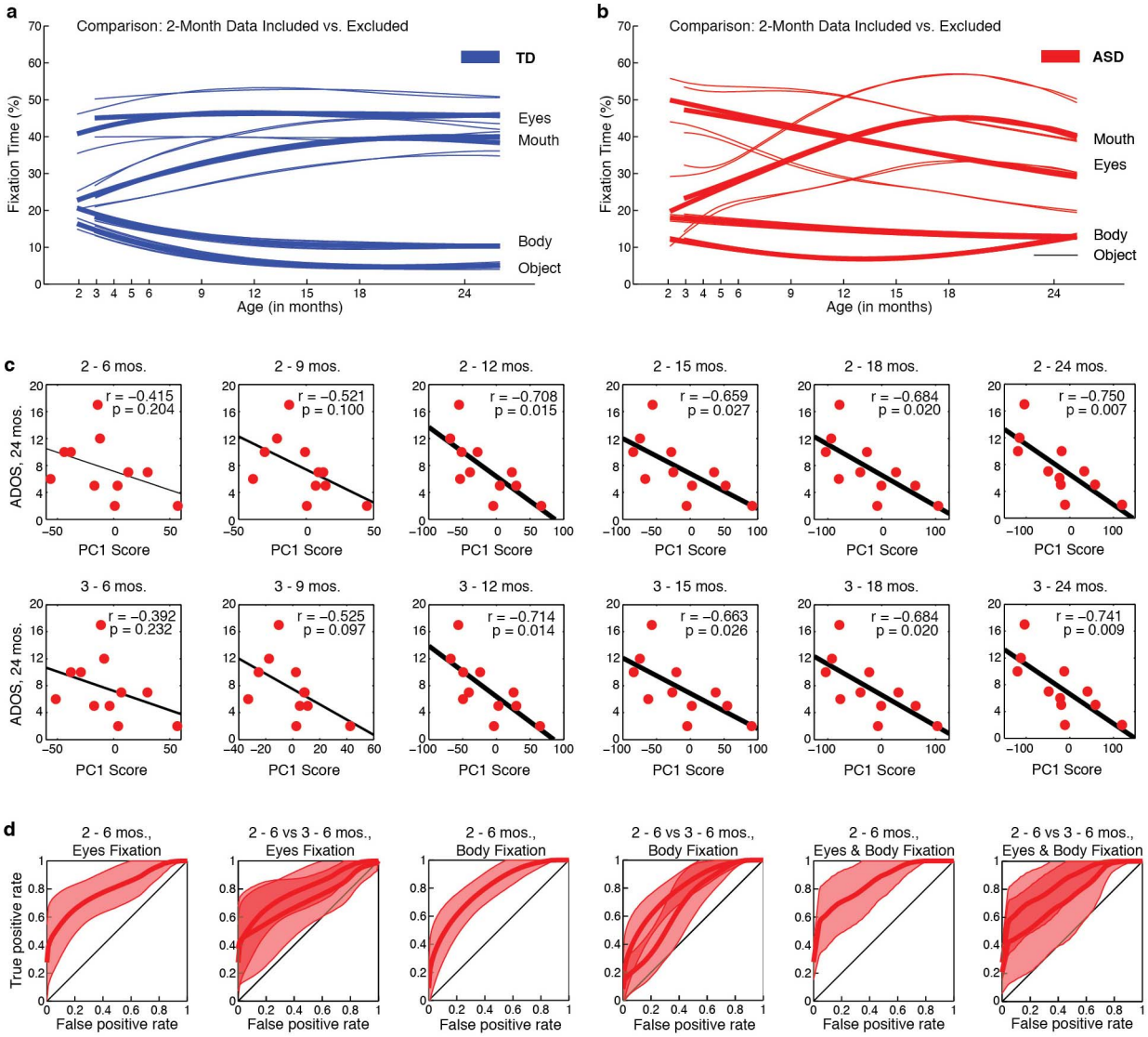

Extended Data Figure 9 | Growth charts of social visual engagement and their relationship to dimensional and categorical outcome, with data from month 2 included versus excluded. **a**–**d**, Comparison of growth curves with month 2 data included or excluded for **a**, typically developing males (TD, in blue) and, **b**, for males with an ASD (in red). Exclusion of the month-2 data does not significantly alter the trajectories themselves, and it does not alter the between-group comparisons. **c**, Outcome levels of social disability (as measured by ADOS social-affect score) as a function of decline in eyes fixation (measured as eyes PC1 score, as in Extended Data Fig. 1) using subsets of the longitudinal data (that is, decline in eye fixation using only data collected from month 2 to 6 or 3 to 6, excluding data thereafter; then from months 2 to 9 or 3 to 9, and so on). In the top row, month-2 data are included; in the bottom row, month-2 data are excluded. When month-2 data are included or excluded, decline in eye fixation still significantly predicts future outcome; this relationship reaches trend level significance by the developmental period from months 3 to 9 ($P = 0.097$), and is statistically significant thereafter (with $r = -0.714$, $P = 0.014$ for 3 to 12 months). **d**, ROC curves for comparison of overlap in values between infants with confirmed ASD outcomes relative to typically developing infants. Using leave-one-out cross-validation, plots show mean and 95% confidence intervals for comparison of overlap in values based on change in eye fixation (first two plots from left), change in body fixation (middle two plots), and change in both eye and body fixation (last two plots at right) between 2 and 6 months of age. Plots show ROC for comparison of overlap in values using data from months 2 to 6 and for the comparison of month 2 to 6 relative to month 3 to 6. With month-2 data excluded, confidence intervals for the cross-validated ROC curves increase in size (as expected, in proportion to the reduction in data by excluding month 2), but the curves remain significantly different from chance, and the ROC curves with month-2 data included or excluded are not significantly different from one another.

Extended Data Table 1 | Parameter values and regions of interest

a

	Model	Group	Intercept (s.e.m.)	Age coefficient B_1 (s.e.m.)	Age coefficient B_2 (s.e.m.)	Age coefficient B_3 (s.e.m.)
Eyes	3rd order	TD	13.410 (19.009)	9.6878 (4.5920)	-0.7919 (0.3801)	0.0179 (0.0092)
	3rd order	ASD	66.979 (8.665)	-3.5843 (2.0843)	0.0817 (0.1726)	0.0001 (0.0042)
Mouth	2nd order	TD	11.411 (13.269)	3.6110 (1.6954)	-0.0917 (0.0537)	n.a.
	2nd order	ASD	-6.596 (6.081)	6.7058 (0.7762)	-0.1977 (0.0244)	n.a.
Body	Inverse	TD	6.872 (5.162)	45.6250 (28.3084)	n.a.	n.a.
	Inverse	ASD	13.450 (2.358)	12.8734 (12.9730)	n.a.	n.a.
Object	3rd order	TD	32.772 (8.973)	-5.7665 (2.3918)	0.3570 (0.1980)	-0.0068 (0.0048)
	3rd order	ASD	17.366 (4.100)	-1.4479 (1.0913)	0.0201 (0.0904)	0.0014 (0.0022)

s.e.m. = standard error measure

b

	Group	w_μ[1]	w_G[2]	Eigenfunctions[3]	FVE
Eyes	TD	5.7045	[2.5422, 2.5422]	2	96.48%, 3.49%
	ASD	6.3868	[2.2335, 2.2335]	3	82.72%, 10.66%, 6.18%
Mouth	TD	5.6800	[2.5431, 2.5431]	2	94.06%, 5.93%
	ASD	6.3879	[2.2339, 2.2339]	3	69.89%, 20.95%, 8.98%
Body	TD	5.6729	[2.5415, 2.5415]	2	91.75%, 8.19%
	ASD	6.3894	[2.2339, 2.2339]	2	98.71%, 1.28%
Object	TD	5.6935	[2.5433, 2.5433]	2	91.14%, 8.85%
	ASD	6.3883	[2.2331, 2.2331]	2	95.25%, 4.25%

[1] Bandwidth for mean function, w_μ, selected by generalized cross-validation.
[2] Bandwidth for covariance surface, w_G, selected by generalized cross-validation.
[3] Number of eigenfunctions selected by Akaike Information Criterion (AIC).
FVE = Fraction of Variance Explained

c

	Eyes	Mouth	Body	Object
Horizontal[1]	8.04° (0.46)	7.71° (0.49)	25.11° (2.70)	31.99° (0.05)[2]
Vertical[1]	6.91° (0.44)	5.72° (0.59)	21.71° (0.73)	23.94° (0.49)[2]

[1] Data are given as mean (SD) in degrees of visual angle.
[2] Object ROIs generally spanned the full horizontal and vertical extent of the background in all video images, excepting cases of some body and hand gestures, as shown in Figure 1 in the main text. The average minimum visual area subtended by any portion of the object ROI is equal to the difference between object and body ROIs.

a, Table of parameter values for hierarchical linear modelling. **b**, Table of parameter values for PACE/FDA smoothing bandwidths, eigenfunctions, and fraction of variance explained (FVE). **c**, Table of sizes of regions of interest in video stimuli.